scientific reports



OPEN

Serum extracellular vesicles containing adenoviral E1A-DNA as a predictive biomarker for liquid biopsy in oncolytic adenovirus therapy

Chiaki Yagi¹, Shinji Kuroda¹, Yoshihiko Kakiuchi¹, Shunya Hanzawa¹, Daisuke Kadowaki¹, Yusuke Yoshida¹, Masaki Sakamoto¹, Yuki Hamada¹, Ryoma Sugimoto¹, Tomoko Ohtani¹, Kento Kumon¹, Masashi Hashimoto¹, Nobuhiko Kanaya¹, Satoru Kikuchi¹, Shunsuke Kaqawa¹, Hiroshi Tazawa¹, Yasuo Urata² & Toshiyoshi Fujiwara¹

Oncolytic adenoviruses replicate selectively in tumor cells and induce immunogenic cell death, but predictive biomarkers for early therapeutic response are lacking. This study evaluated extracellular vesicle-encapsulated adenoviral E1A-DNA (EV-E1A-DNA) as a minimally invasive biomarker for monitoring responses to telomerase-specific oncolytic adenoviruses OBP-301 and OBP-502. EVs were isolated from human and murine cancer cell lines and from the serum of treated mice using ultracentrifugation. EV-associated E1A-DNA levels were measured by quantitative polymerase chain reaction and found to correlate with cytotoxicity in vitro and tumor regression in vivo. In xenograft models, serum EV-E1A-DNA levels at 2 days post-treatment showed strong correlations with final tumor volume and survival, supporting their utility as an early predictive biomarker. In immunocompetent mice pre-immunized with wild-type adenovirus, free viral DNA was undetectable in serum due to neutralizing antibodies, whereas EV-E1A-DNA remained detectable. This "stealth effect" indicates that EVs protect viral components from immune clearance. These results demonstrate that EV-E1A-DNA is a sensitive and virus-specific biomarker that enables early assessment of therapeutic efficacy, even in the presence of antiviral immunity. This strategy offers a promising liquid biopsy approach for personalized monitoring of oncolytic virotherapy and may be applicable to other virusbased therapies.

Keywords Oncolytic adenovirus, Extracellular vesicle, Liquid biopsy, Predictive biomarker, Stealth effect.

Predictive biomarkers play a crucial role in cancer treatment by identifying patients most likely to respond to specific therapies, enabling personalized treatment strategies. Circulating tumor DNA (ctDNA), a key component of liquid biopsy, has attracted attention as a promising biomarker that provides real-time, non-invasive insights into treatment response and the emergence of resistant mutations, enabling early detection of genetic alterations and timely therapeutic adjustments^{1,2}. Extracellular vesicles (EVs), including exosomes, microvesicles, and apoptotic bodies, have also been recognized as important biomarkers due to their ability to carry tumor-derived molecular components such as proteins, nucleic acids, and lipids that reflect the characteristics of cancer cells^{3–5}. EVs originate primarily from endosomal multivesicular bodies (MVBs), which fuse with the plasma membrane and release their contents into the extracellular environment. Their role in intercellular communication and their capacity to provide dynamic information about the tumor microenvironment make them promising tools for monitoring disease progression and therapeutic efficacy. As EVs circulate in bodily fluids, including blood and urine, they serve as a crucial component of liquid biopsy, offering a minimally invasive approach to tumor profiling and treatment monitoring⁶. Notably, EVs can function as carriers of viral DNA; for instance, hepatitis

¹Department of Gastroenterological Surgery, Dentistry and Pharmaceutical Sciences, Okayama University Graduate School of Medicine, 2-5-1 Shikata-cho, Kita-ku, Okayama 700-8558, Japan. ²Oncolys BioPharma, Inc., Tokyo, Japan. [⊠]email: shinkuro@okayama-u.ac.jp

B virus (HBV) DNA transmitted via EVs is resistant to antibody neutralization, a phenomenon known as the "stealth effect".

Oncolytic virus therapy is an emerging cancer treatment that leverages genetically engineered viruses to selectively infect and replicate within tumor cells, causing their destruction while stimulating antitumor immune responses⁸. Several oncolytic viruses, including talimogene laherparepvec (T-VEC) and teserpaturev, have been approved for clinical use, and ongoing research is exploring their combination with immunotherapies and other standard treatments to enhance therapeutic efficacy^{9,10}. We have developed telomerase-specific oncolytic adenoviruses, including suratadenoturev (OBP-301)¹¹⁻¹³. OBP-301 is currently being evaluated in multiple clinical trials for various solid tumors, including esophageal, gastric, and hepatocellular carcinomas¹⁴. These trials are investigating its safety and efficacy as monotherapy and in combination with standard treatments such as radiation therapy and immune checkpoint inhibitors (ICIs)^{15,16}. In relation to EVs, our previous preclinical study in mice demonstrated that, in addition to activating antitumor immune responses, tumor-derived EVs also play an important role in the abscopal effect induced by local OBP-301 therapy^{17,18}. This study showed that OBP-301 or its components, such as proteins and nucleic acids, are released from tumors while encapsulated in tumor-derived EVs, allowing these EVs to transport OBP-301 to distant metastatic sites, where they exert a therapeutic effect (abscopal effect).

In the present study, based on the hypothesis that greater proliferation of OBP-301 within the tumor and an enhanced therapeutic effect lead to greater release of OBP-301 or its components encapsulated in tumor-derived EVs into the bloodstream, the usefulness of liquid biopsy targeting adenoviral E1A-DNA, one of the components of OBP-301 encapsulated in tumor-derived EVs and released from OBP-301-treated tumor cells, as a predictive biomarker for OBP-301 therapy was investigated. The concept of using the DNA of the therapeutic virus, rather than patient-derived DNA, as a predictive biomarker is an innovative and unprecedented approach, which appears to be a distinctive feature of oncolytic virus therapy as a biological agent. The findings of this study are expected to pave the way for the development of personalized medicine in oncolytic virus therapy.

Results

Oncolytic adenoviruses are encapsulated within EVs and secreted

Transmission electron microscopy (TEM) demonstrated that, though EVs were observed in multivesicular bodies (MVBs) in HCT116 cells, viral particles were detected within EVs in HCT116 cells treated with OBP-301 (Fig. 1A). These viral particles were secreted into the culture media encapsulated within EVs, although free, non-encapsulated viruses were also detected in the surrounding environment (Fig. 1B). Dynamic light scattering (DLS) showed that both control EVs and EVs collected after OBP-301 treatment (301-EVs) were approximately 100 nm in size across all human colon carcinoma cell lines (HCT116, SW480, HT29, and RKO) (Fig. 1C). Western blot analysis of EVs demonstrated that, though CD9 and CD81, representative EV markers, were detected in both control EVs and 301-EVs from all cell lines, adenoviral E1A protein expression was observed only in 301-EVs. The strongest E1A expression was found in HCT116, followed by SW480 and HT29, with minimal expression in RKO (Fig. 1D, Supplementary Fig. S1A). When the amount of E1A-DNA in both intracellular EVs and EVs present in the culture supernatant was measured after OBP-301 treatment, focusing on HCT116 (which showed high E1A expression in EVs) and RKO (which showed weak expression), high levels of E1A-DNA were detected in both intracellular and supernatant EVs in HCT116, whereas both were low in RKO, demonstrating a correlation (Fig. 1E). A similar evaluation using the murine pancreatic cancer cell line PAN02 and the mouse-adapted OBP-301 variant, OBP-502, showed that viral particles were detected within EVs collected after OBP-502 treatment (502-EVs). The 502-EVs, approximately 100 nm in size, also contained E1A proteins (Fig. 1F-H, Supplementary Fig. S1B). These findings suggest that oncolytic viral particles and their components are secreted encapsulated within EVs following treatment, and that the amounts of virus and its components vary among cell lines.

Extracellular vesicle-encapsulated E1A-DNA levels are significantly correlated with the cytotoxicity of OBP-301 in vitro

To examine the correlation between differences in extracellular vesicle-encapsulated E1A-DNA (EV-E1A-DNA) levels and the therapeutic efficacy of OBP-301, HCT116, SW480, HT29, and RKO cells were treated with various doses of OBP-301, and the levels of EV-E1A-DNA released into the culture supernatant were measured by polymerase chain reaction (PCR). In HCT116, SW480, and HT29 cells, the amount of EV-E1A-DNA increased proportionally to both the occurrence and magnitude of the therapeutic effect. In contrast, in RKO cells, in which little to no therapeutic effect was observed, EV-E1A-DNA was also barely detectable (Fig. 2A). Similarly, when the correlation between EV-E1A-DNA levels and the therapeutic efficacy of OBP-301 was evaluated over time in these cell lines, a consistent correlation was observed (Fig. 2B). A similar correlation between the therapeutic efficacy of OBP-502 and EV-E1A-DNA levels was observed in PAN02 cells (Fig. 2C, D).

To address the concern that the observed correlation might be due to the presence of free viruses rather than EVs, since the material collected by ultracentrifugation may contain both EVs and free viruses, an additional analysis was performed using ExoCap, a reagent specifically designed for the isolation of EVs, including exosomes, after ultracentrifugation. Although the EV-E1A-DNA levels decreased compared with ultracentrifugation alone, the correlation with therapeutic efficacy remained evident, which is particularly important in in vivo studies in which neutralizing antibodies against adenoviruses are present (Supplementary Fig. S2). These findings suggest that EV-E1A-DNA levels are significantly correlated with the therapeutic effects of oncolytic adenoviruses, indicating their potential as a predictive biomarker.

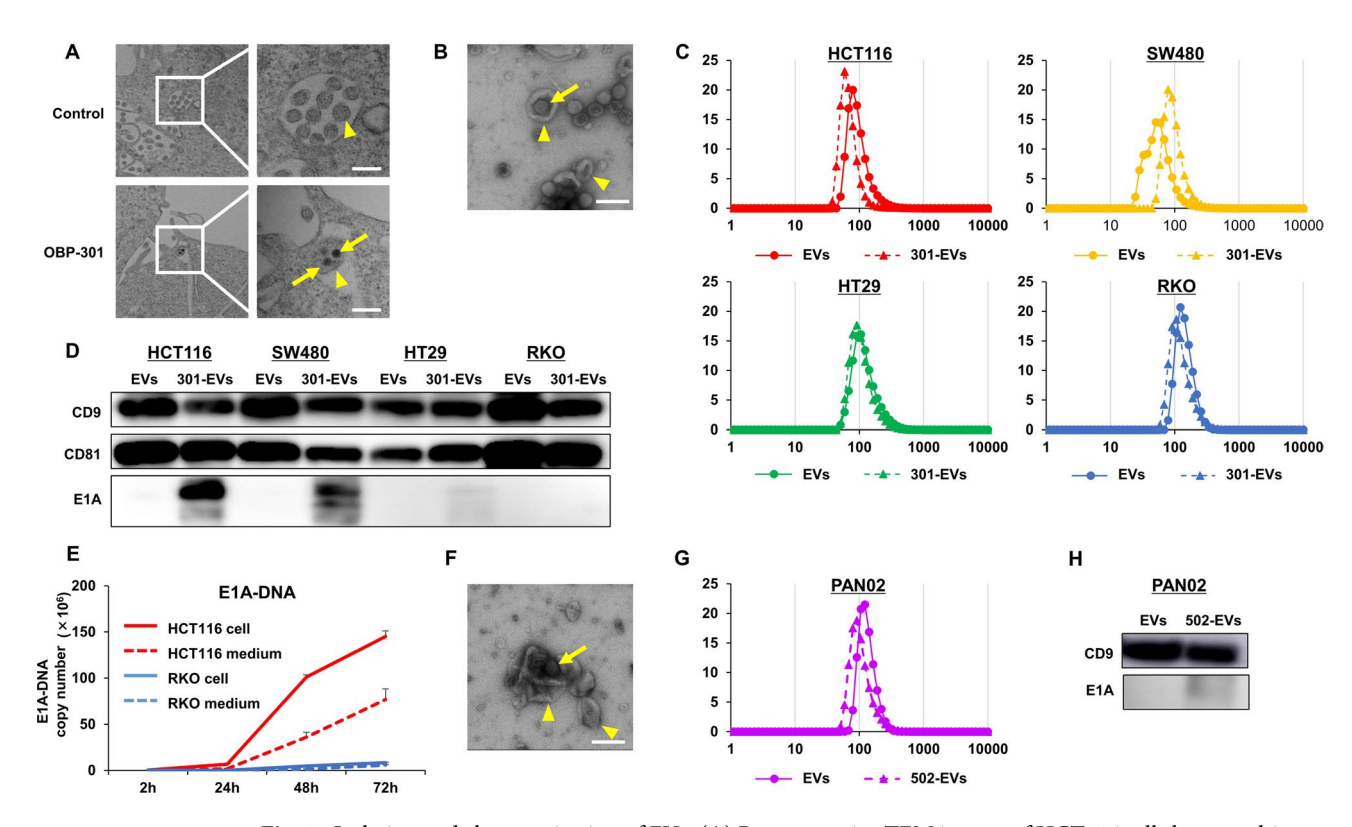


Fig. 1. Isolation and characterization of EVs. (**A**) Representative TEM images of HCT116 cells harvested 2 days after treatment with PBS (control) or OBP-301 (50 MOI). The right panel shows a magnified view of the area outlined by the box in the left panel. Yellow arrows indicate viral particles, and yellow arrowheads indicate EVs. Scale bar, 200 nm. (**B**) Representative TEM images of 301-EVs isolated from the culture media of HCT116 cells. Yellow arrows indicate viral particles, and yellow arrowheads indicate EVs. Scale bar, 200 nm. (**C**) Particle size of EVs and 301-EVs isolated from the culture media of HCT116, SW480, HT29, and RKO cells, measured by dynamic light scattering (DLS). (**D**) Western blot analysis (cropped, full-length blot images in Supplementary Fig. S1A) of CD9, CD81, and E1A in EVs and 301-EVs isolated from the culture media of HCT116, SW480, HT29, and RKO cells. (**E**) qPCR analysis of E1A-DNA in cells or the culture media of HCT116 and RKO cells collected 2, 24, 48, or 72 h after OBP-301 treatment (50 MOI) (n=3). (**F**) Representative TEM image of 502-EVs isolated from the culture media of PAN02 cells. Yellow arrows indicate viral particles, and yellow arrowheads indicate EVs. Scale bar, 200 nm. (**G**) Particle size of EVs and 502-EVs isolated from the culture media of PAN02 cells, measured by DLS. (**H**) Western blot analysis (cropped, full-length blot images in Supplementary Fig. S1B) of CD9 and E1A in EVs and 502-EVs isolated from the culture media of PAN02 cells.

Early-phase serum EV-E1A-DNA levels are significantly correlated with the final antitumor effects of OBP-301 in immunodeficient mice

When the antitumor effects of OBP-301 against HCT116 and RKO subcutaneous tumors were evaluated in immunodeficient BALB/c nude mice, a single intratumoral injection of OBP-301 significantly suppressed the growth of HCT116 tumors, whereas no effects were observed in RKO tumors, consistent with the in vitro findings (Fig. 3A). After confirming that EVs could be isolated from mouse blood samples using ultracentrifugation, OBP-301 was administered via intratumoral injection in the HCT116 and RKO subcutaneous tumor models, and EVs were extracted from blood samples collected 2 days after treatment (Supplementary Fig. S3A). Consistent with the in vitro results, apart from free virus, EVs containing internalized viral particles were detected in HCT116 tumors by TEM, whereas few such EVs were observed in RKO tumors (Fig. 3B). When serum EV-E1A-DNA levels were monitored by PCR up to 7 days after OBP-301 intratumoral injection in HCT116 and RKO tumors, serum EV-E1A-DNA levels increased over time in HCT116 tumors, whereas they remained largely unchanged in RKO tumors (Fig. 3C). To assess the relationship between early EV-E1A-DNA levels and therapeutic outcomes, the correlations between the final tumor volume, measured 28 days after a single intratumoral injection of OBP-301 in HCT116 tumors, and serum EV-E1A-DNA levels collected at 2, 7, and 14 days after treatment were analyzed (Supplementary Fig. S3B). EV-E1A-DNA levels collected 2 days after treatment showed the strongest correlation with final tumor volume (r = -0.85, p = 0.018), compared with those collected at 7 days (r = 0.29, p = 0.52) and 14 days (r = 0.55, p = 0.20) (Fig. 3D). These findings suggest that serum EV-E1A-DNA levels reflect the therapeutic effects of OBP-301 in vivo. Notably, the observation that EV-E1A-DNA levels at the early time point of day 2 after treatment were the most predictive of therapeutic efficacy is of particular significance.

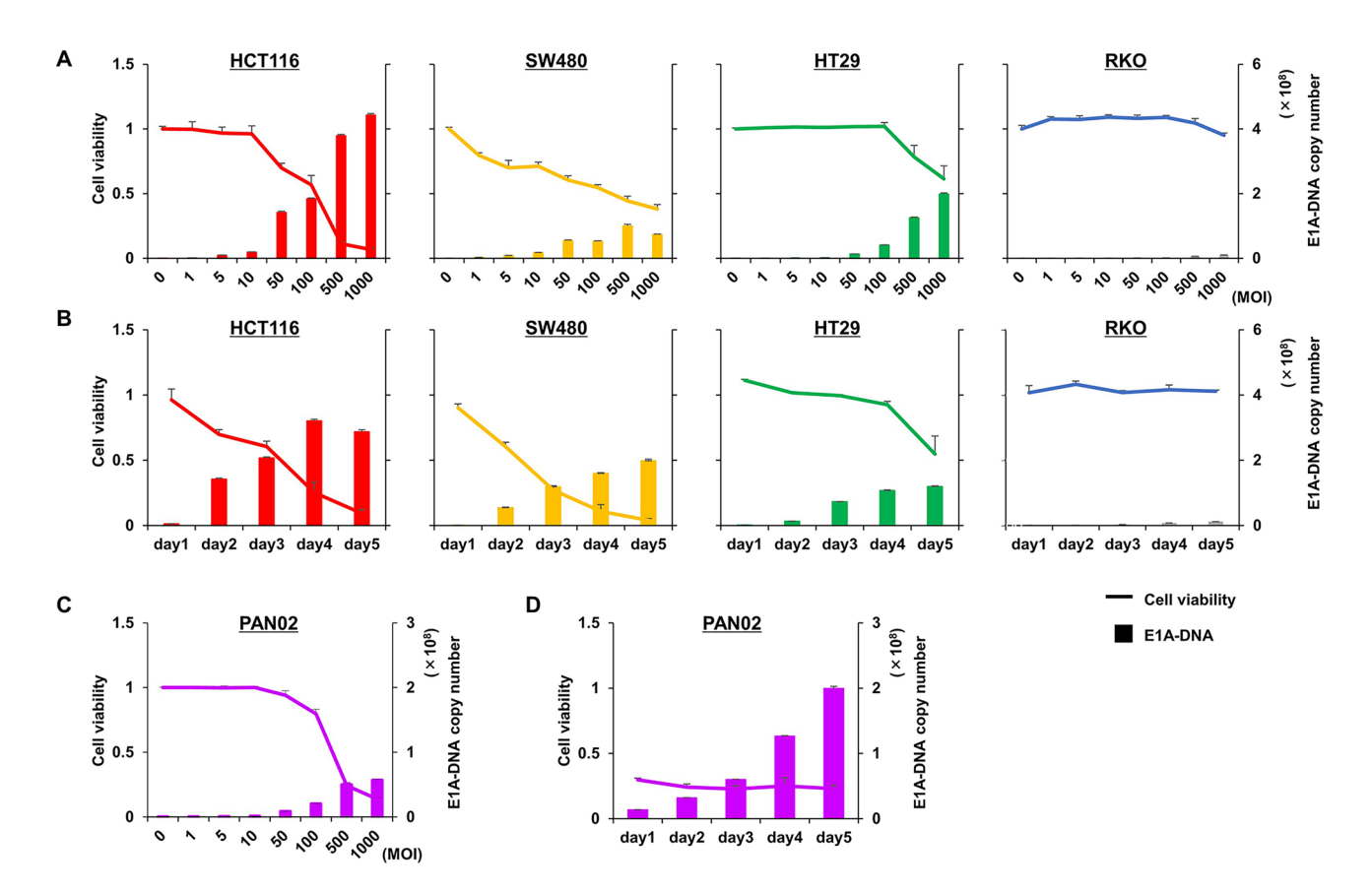


Fig. 2. Correlation between OBP-301 cytotoxicity and EV-E1A-DNA levels in vitro. (**A**) Cell viability (line graph) was assessed in HCT116, SW480, HT29, and RKO cells 2 days after OBP-301 treatment at the indicated doses (n = 5). E1A-DNA levels (bar graph) in EVs isolated from the culture media in the same experiment were measured by qPCR. (**B**) Cell viability (line graph) was assessed in HCT116, SW480, HT29, and RKO cells at the indicated time points after OBP-301 treatment (50 MOI) (n = 5). E1A-DNA levels (bar graph) in EVs isolated from the culture media in the same experiment were measured by qPCR. (**C**) Cell viability (line graph) was assessed in PAN02 cells 2 days after OBP-502 treatment at the indicated doses (n = 5). E1A-DNA levels (bar graph) in EVs isolated from the culture media in the same experiment were measured by qPCR. (**D**) Cell viability (line graph) was assessed in PAN02 cells at the indicated time points after OBP-502 treatment (500 MOI) (n = 5). E1A-DNA levels (bar graph) in EVs isolated from the culture media in the same experiment were measured by qPCR.

Serum EV-E1A-DNA serves as a predictive biomarker of OBP-301 in immunocompetent mice possessing anti-adenoviral antibodies

OBP-301 and OBP-502 are based on human adenovirus type 5, a prevalent cause of the common cold. As a result, most adults already possess neutralizing antibodies against this virus, causing free virus released into the bloodstream after intratumoral injection to be rapidly captured and cleared by antibody-mediated adaptive immunity. This makes it difficult to use free virus as a predictive biomarker. To generate mice with neutralizing antibodies against adenoviruses, immunocompetent C57BL/6 mice were injected twice with wild-type adenovirus at one-week intervals, and blood samples were collected 2, 3, and 4 weeks after the initial injection (Supplementary Fig. S4A). The presence of neutralizing antibodies in the blood was indirectly assessed using OBP-401, a green fluorescent protein (GFP)-expressing oncolytic adenovirus. When culture medium supplemented with blood collected two weeks after the initial injection was used, OBP-401 infection of HCT116 cells was significantly inhibited, suggesting the presence of neutralizing antibodies (Fig. 4A). A similar level of neutralizing antibodies was also confirmed in blood samples collected three and four weeks after the initial injection.

In a C57BL/6 mouse model vaccinated with wild-type adenovirus one or two weeks before PAN02 subcutaneous tumor inoculation, blood samples were collected over time after OBP-502 intratumoral injection, and E1A-DNA levels in both serum and EVs isolated by ultracentrifugation were measured by PCR (Supplementary Fig. S4B). Whereas no significant E1A-DNA was detected in serum, a significant increase was observed in EVs collected on days 2 and 3 after OBP-502 administration, demonstrating the stealth effect of EVs (Fig. 4B). In the vaccinated C57BL/6 mouse model bearing PAN02 subcutaneous tumors, the correlation between the final therapeutic effect of a single OBP-502 injection (day 28) and serum EV-E1A-DNA levels collected on days 2, 7, and 14 after treatment was evaluated (Supplementary Fig. S4C). The strongest correlation was observed on day 2 (r = -0.79, p = 0.031), compared with days 7 (r = -0.28, p = 0.54) and 14 (r = 0.01, p = 0.97), consistent with the in vitro results

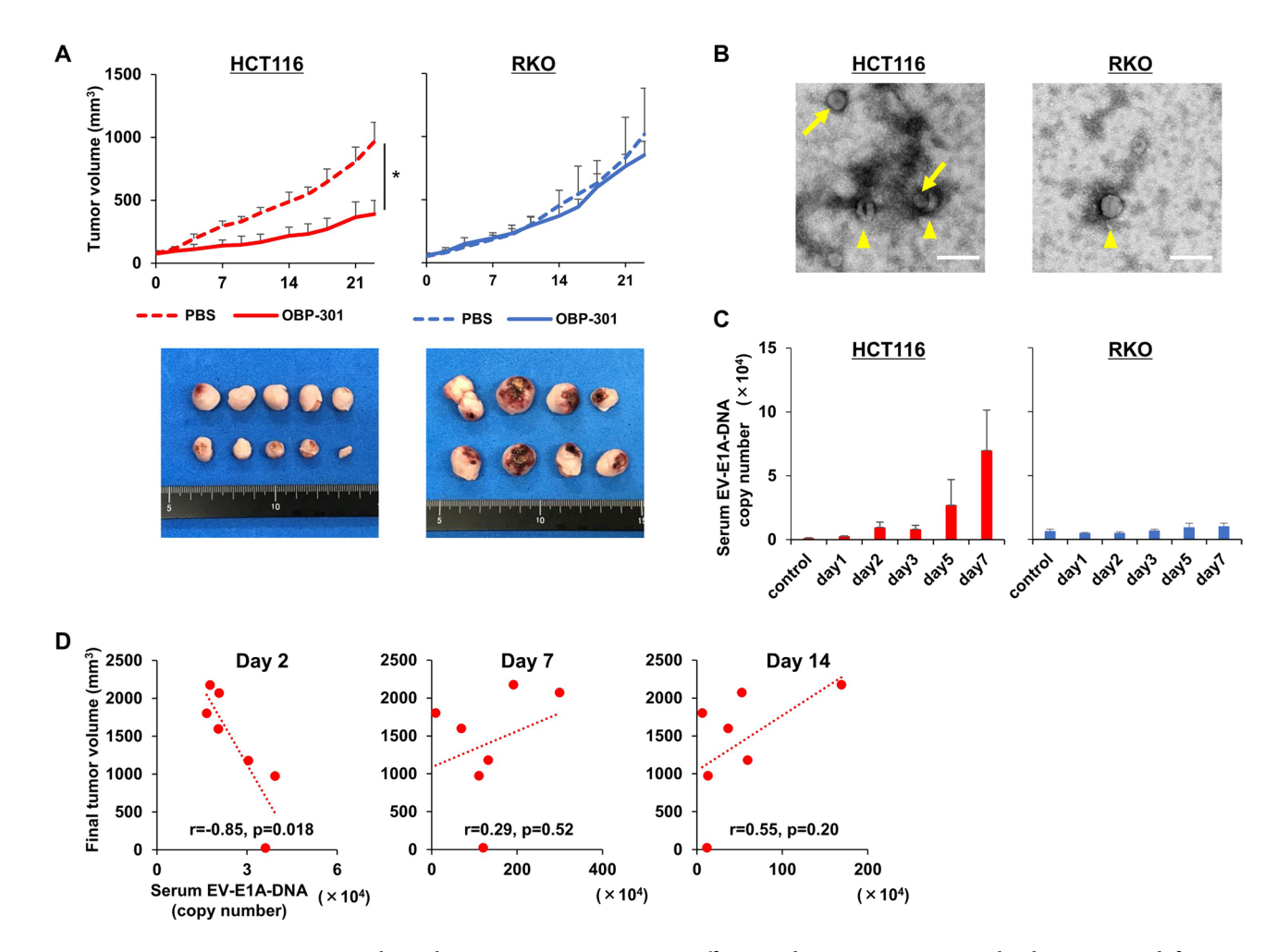


Fig. 3. Correlation between OBP-301 antitumor efficacy and serum EV-E1A-DNA levels in immunodeficient mice. (**A**) HCT116 (n=5) and RKO (n=4) subcutaneous tumors inoculated into immunodeficient BALB/c nude mice were intratumorally treated once with PBS or OBP-301 (1.0×10^8 PFUs), and tumor volumes were monitored for up to 23 days after treatment. The bottom images show the macroscopic appearance of tumors harvested on day 23. *p<0.001. (**B**) Representative TEM images of EVs isolated from the serum of mice bearing HCT116 or RKO subcutaneous tumors collected 2 days after OBP-301 treatment (1.0×10^8 PFUs). Scale bar, 200 nm. (**C**) BALB/c nude mice bearing HCT116 or RKO subcutaneous tumors were intratumorally treated once with OBP-301 (1.0×10^8 PFUs), and sacrificed at 1, 2, 3, 5, and 7 days after treatment. Whole blood was collected each day, and E1A-DNA levels in serum EVs were measured by qPCR (n=3). (**D**) In BALB/c nude mice bearing HCT116 subcutaneous tumors, which were intratumorally treated once with OBP-301 (1.0×10^8 PFUs), blood samples (200 μL) were collected on days 2, 7, and 14 after treatment, and tumor volumes were monitored until day 28 (n=7). Correlations between serum EV-E1A-DNA levels at each time point and the final tumor volume on day 28 were analyzed.

(Fig. 4C). Furthermore, serum EV-E1A-DNA levels collected on day 2 were significantly correlated with survival (r=0.80, p=0.018), based on the criterion that mice were considered to have reached the experimental endpoint when tumor volume exceeded 150 mm³ (Fig. 4D). Serum EV-E1A-DNA levels were also significantly correlated with E1A-DNA levels in the tumor (r=0.93, p<0.001) (Fig. 4E, Supplementary Fig. S4D). These findings suggest that serum EV-E1A-DNA levels measured on day 2 serve as a useful biomarker for predicting the therapeutic efficacy of oncolytic adenoviruses, even in the presence of neutralizing antibodies, highlighting their potential for clinical application.

Discussion

Several features make EVs particularly suitable as predictive biomarkers in cancer therapy. First, EVs are highly stable in biological fluids such as blood, urine, and saliva, which allows for robust, non-invasive sampling and longitudinal monitoring¹⁹. Furthermore, EVs provide dynamic and real-time insights into tumor biology because their contents reflect the molecular characteristics of tumor cells, including genetic mutations and treatment-induced changes. Second, EVs have the potential to enhance detection sensitivity compared with direct analysis of whole serum²⁰. Biomolecules of interest, such as tumor-derived genomic DNA and proteins, may be present in low abundance or masked by background signals in serum. In contrast, EVs can selectively enrich and

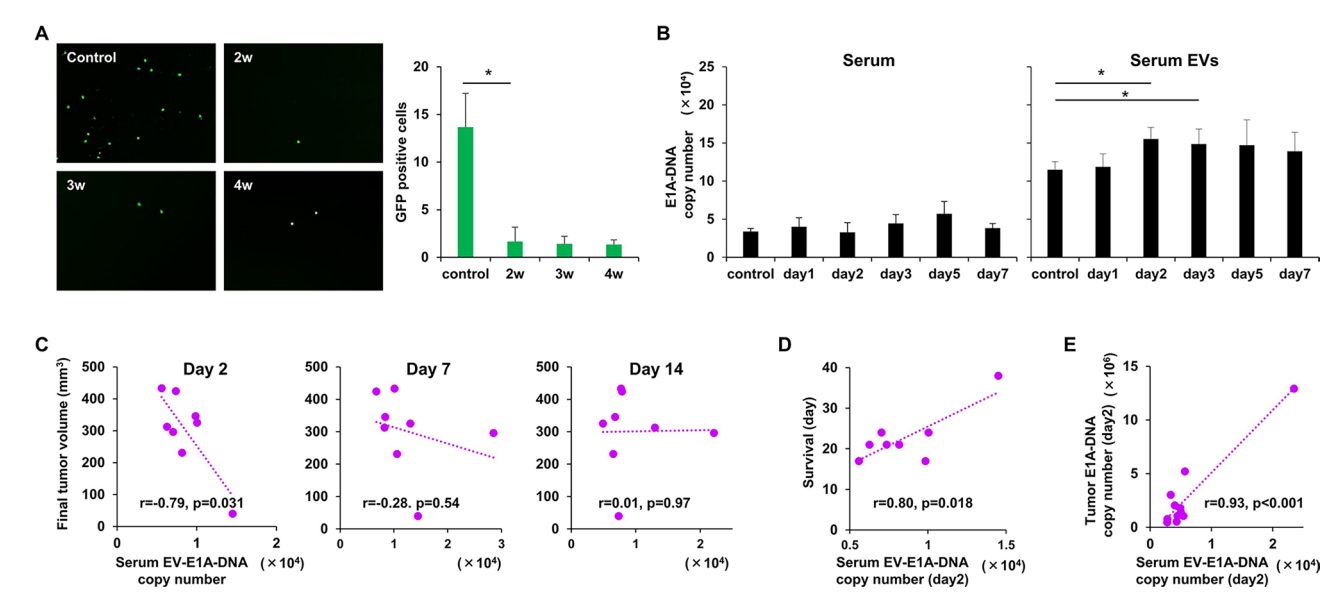


Fig. 4. Correlation between OBP-502 antitumor efficacy and serum EV-E1A-DNA levels in immunocompetent mice vaccinated with wild-type adenovirus. (A) C57BL/6 mice were subcutaneously injected twice with wild-type adenovirus type 5 $(1.0 \times 10^9 \text{ PFUs})$ on days 1 and 8 (n = 3 - 4), and whole blood was collected on days 15, 22, and 29. HCT116 cells $(5.0 \times 10^2 \text{ cells/well in a 96-well plate})$ were treated with OBP-401 (1 MOI) for 3 days in the presence of serum diluted 1,024-fold, and GFP-positive spots were observed using a fluorescence microscope. *p < 0.001. (B) Adenovirus-vaccinated C57BL/6 mice bearing PAN02 subcutaneous tumors were intratumorally treated once with OBP-502 (1.0×10^8 PFUs), sacrificed 1, 2, 3, 5, and 7 days after treatment, and whole blood samples were collected each day. The control group was defined as untreated tumor-bearing mice. E1A-DNA levels in serum and serum EVs were measured by qPCR (n = 3-4). *p < 0.001. (C) In adenovirus-vaccinated C57BL/6 mice bearing PAN02 subcutaneous tumors, which were intratumorally treated once with OBP-502 (1.0×10^8 PFUs), blood samples (200 μ L) were collected on days 2, 7, and 14 after treatment, and tumor volumes were monitored until day 28 (n = 8). Correlations between serum EV-E1A-DNA levels at each time point and the final tumor volume on day 28 were evaluated. (D) In the same experiment as in (C), the correlation between serum EV-E1A-DNA levels on day 2 and survival was evaluated, assuming mice were considered to have reached the experimental endpoint when tumor volume exceeded 150 mm³. (E) Adenovirus-vaccinated C57BL/6 mice bearing PAN02 subcutaneous tumors were sacrificed 2 days after intratumoral treatment with OBP-502 $(1.0 \times 10^8 \text{ PFUs})$, and tumors and whole blood samples were collected. E1A-DNA levels in tumors and serum EVs were measured by qPCR (n=3).

protect these components, thereby improving the signal-to-noise ratio and enabling more sensitive and specific detection of tumor-associated changes. This enrichment effect is particularly valuable when analyzing low-copy targets or in early-stage disease, where circulating biomarkers are scant. This characteristic was demonstrated in the present study (Fig. 4B), in which adenoviral E1A-DNA, as the biomarker of interest, was clearly detected in serum EVs collected after oncolytic adenovirus treatment, whereas no significant E1A-DNA signal was detected in whole serum. The modest signal-to-noise ratio observed in Fig. 4B may be related to the limited replication efficiency of human adenovirus in murine cells compared with human cells, although therapeutic efficacy was indeed observed in murine tumors, as shown in (Fig. 2C).

The present study demonstrated that adenoviral E1A-DNA encapsulated in EVs can serve as a robust and minimally invasive predictive biomarker for the efficacy of oncolytic adenovirus therapy. By integrating in vitro and in vivo experimental models, including both immunodeficient and immunocompetent mice, EVs encapsulating viral DNA were shown to be secreted in response to OBP-301 or OBP-502 treatment, and their levels correlated strongly with therapeutic outcomes. These findings highlight the utility of EV-based liquid biopsy in monitoring and predicting responses to oncolytic virotherapy, even in the presence of pre-existing anti-adenoviral immunity. One of the key observations in the present study is that EV-E1A-DNA levels reflect the extent of viral replication and cytotoxicity across multiple human colon cancer cell lines, as well as in murine pancreatic cancer cells. This correlation was consistently observed in both dose- and time-dependent settings. Importantly, these findings were further validated in vivo, in which serum EV-E1A-DNA levels collected after a single intratumoral injection of OBP-301 or OBP-502 correlated strongly with final tumor volumes and survival. Notably, serum EV-E1A-DNA levels as early as day 2 post-treatment showed the highest predictive value, suggesting that this biomarker may be useful for early therapeutic decision-making.

A particularly novel aspect of the present study is the demonstration that EVs enable viral components to evade neutralizing antibodies, an immunological barrier that often limits the systemic efficacy and detectability of oncolytic viruses. In immunocompetent mice vaccinated with wild-type adenovirus, free E1A-DNA was undetectable in serum, whereas EV-E1A-DNA remained readily measurable. This "stealth effect" is consistent with prior findings in other viral systems, such as hepatitis B virus, and supports the hypothesis that EVs can

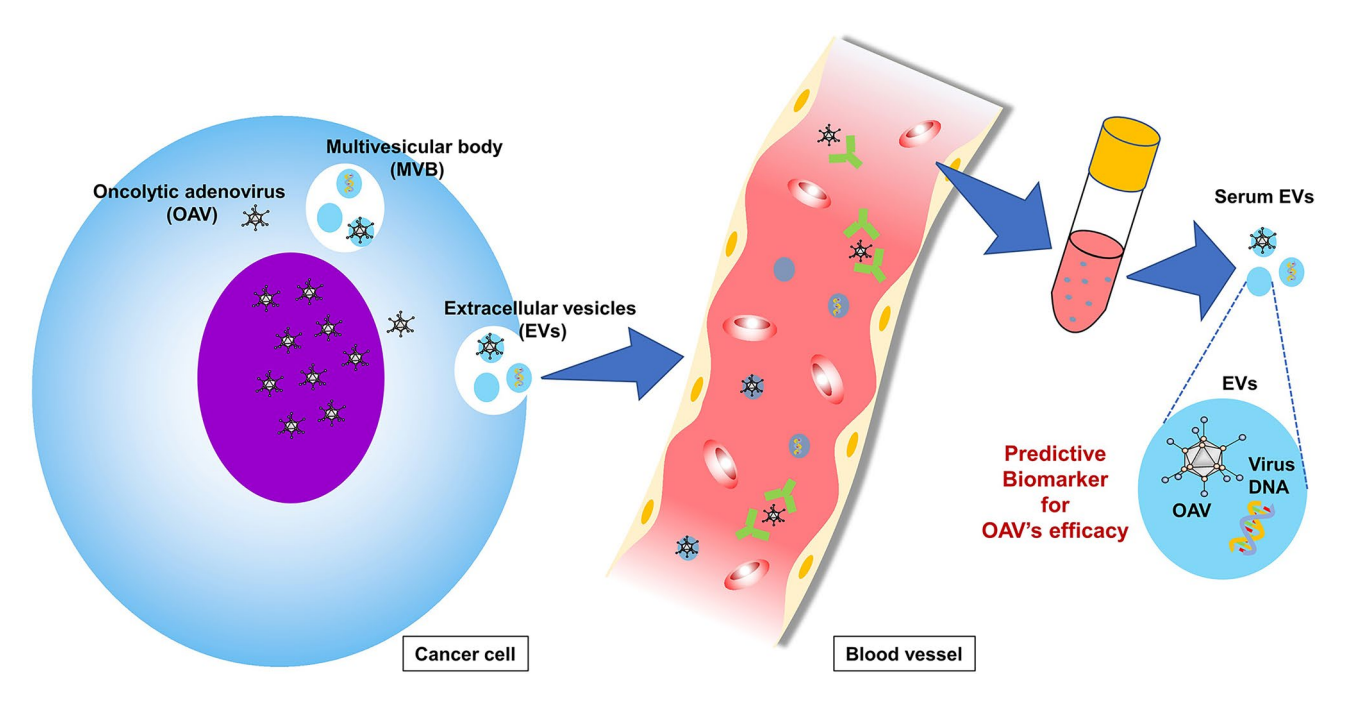


Fig. 5. Schematic Illustration.

protect and stabilize viral nucleic acids in circulation. These findings provide a new mechanistic insight into the immune-evasive properties of EVs and further support their use in virotherapy monitoring. Clinically, this approach offers several advantages over traditional tumor biopsies or serum-based assays. EVs are stable in biofluids, reflect tumor-specific molecular signatures, and can be repeatedly sampled with minimal invasiveness. Moreover, the use of viral DNA as a biomarker, rather than host-derived ctDNA, represents a novel paradigm that is unique to oncolytic virotherapy and may be generalized to other viral agents engineered for cancer treatment.

This study has several limitations. First, although the correlation between EV-E1A-DNA levels and antitumor efficacy was confirmed in murine models, validation using clinical samples is necessary to establish its predictive value in human patients. Second, whether this correlation will persist following repeated administration of oncolytic viruses or in combination with chemotherapeutic agents, radiation therapy, or ICIs remains unclear. Third, whereas this study focused on E1A-DNA, the potential contribution of other viral or host-derived EV contents, such as proteins and microRNAs, to therapeutic response has yet to be elucidated. Fourth, though ultracentrifugation was used for EV isolation in this study, its limited reproducibility and scalability may restrict clinical applicability. More rapid and standardized methods, such as immunoaffinity capture or size exclusion chromatography, may be required for future clinical use.

In conclusion, the present findings suggest that EV-encapsulated viral DNA represents a novel, sensitive, and non-invasive predictive biomarker for oncolytic adenovirus therapy (Fig. 5). This strategy offers strong potential for clinical implementation in the context of personalized virotherapy, particularly for early response monitoring and overcoming limitations posed by antiviral immunity. Further clinical validation and mechanistic studies are warranted to fully harness the potential of EV-based liquid biopsy in cancer treatment.

Methods

Cell lines and culture conditions

HCT116, SW480, HT29, and RKO, human colon carcinoma cell lines, and PAN02, a murine pancreatic carcinoma cell line, were used in this study. HCT116, SW480, HT29, and RKO cells were purchased from the American Type Culture Collection (ATCC, Manassas, VA, USA), and PAN02 cells were obtained from the National Cancer Institute (Frederick, MD, USA). HCT116 cells were cultured in McCoy's 5 A medium; SW480 and HT29 cells were cultured in DMEM; RKO cells were cultured in MEM; and PAN02 cells were cultured in RPMI 1640 medium. All culture media were supplemented with 10% fetal bovine serum and 1% penicillin-streptomycin (100 U/mL).

Oncolytic adenoviruses

Three different telomerase-specific oncolytic adenoviruses were used in this study (Supplementary Fig. S5). OBP-301, which contains the human telomerase reverse transcriptase (hTERT) promoter driving the expression of the adenoviral E1A and E1B genes, selectively replicates in tumor cells while sparing normal cells, thereby inducing oncolytic cell death. OBP-502, a variant of OBP-301, carries a modified fiber incorporating an RGD peptide to enhance infection of murine tumor cells by interacting with integrin $\alpha v\beta 5$, which is expressed on tumor cells. OBP-401, another OBP-301 variant, is engineered to express GFP in infected cells. Multiplicity

of infection (MOI) and plaque-forming units (PFUs) were used to quantify viral doses in vitro and in vivo, respectively.

EV isolation and characterization

In in vitro experiments, normal EVs were isolated by ultracentrifugation of supernatants collected after culturing cells in FBS-free medium for 48 h (EVs). EVs were also isolated by the same process following OBP-301 or OBP-502 treatment at the indicated doses for 24 h (301-EVs or 502-EVs, respectively). Briefly, the ultracentrifugation protocol involved centrifuging the collected supernatants at $2,000 \times g$ for 10 min to remove cells and debris, followed by filtration through a 0.22- μm filter and centrifugation at $100,000 \times g$ for 70 min at 4 °C (Beckman Ultracentrifuge Optima L-70 K). The resulting pellets were rinsed with phosphate-buffered saline (PBS), subjected to a second ultracentrifugation under the same conditions, and resuspended in PBS.

In in vivo experiments, blood samples were centrifuged sequentially at $1,000 \times g$ for 15 min, $3,000 \times g$ for 20 min, and $12,000 \times g$ for 20 min to remove blood cells and cell fragments, followed by ultracentrifugation at $100,000 \times g$ for 70 min at 4 °C. Subsequent procedures were performed as described for the in vitro experiments.

The morphology and structure of EVs were visualized using a transmission electron microscope (TEM) (H-7560, Hitachi, Japan). The sizes of EVs were measured using dynamic light scattering (DLS) with a Zetasizer Nano ZSP (Malvern Instruments, Malvern, UK). Protein concentrations were determined using the bicinchoninic acid (BCA) assay according to the manufacturer's protocol (Thermo Fisher Scientific, Waltham, MA, USA).

Cell viability assay

HCT116, SW480, HT29, RKO, and PAN02 cells $(4.0 \times 10^3 \text{ cells/well in a 96-well plate}; n = 5)$ were treated with various concentrations of OBP-301 or OBP-502 at different time points. Cell viability was assessed using the Cell Proliferation Kit II (XTT) (Roche, Basel, Switzerland) according to the manufacturer's instructions.

Transmission electron microscopy

For pre-fixation, cell specimens were immersed in 0.1 M PBS (pH 7.4) containing 2% glutaraldehyde and 2% paraformaldehyde for 16–18 h. Post-fixation was performed in 2% osmium tetroxide for 1.5 h. After washing with PBS, the specimens were dehydrated through a graded ethanol series and embedded in low-viscosity resin (Spurr resin; Polysciences, Warrington, PA, USA). Subsequently, 80-nm sections were prepared using an ultramicrotome (EM-UC7; Leica, Tokyo, Japan) and stained with uranyl acetate and lead citrate. The specimens were then examined using an H-7650 microscope.

Western blot analysis

Proteins (20 μ g) were electrophoresed on 10% SDS-polyacrylamide gels and transferred onto Hybond-polyvinylidene difluoride (PVDF) membranes (GE Healthcare UK Ltd., Buckinghamshire, UK). The membranes were incubated overnight at 4 °C with primary antibodies against CD9 (for human) (1:1000; Invitrogen, cat. 10626D), CD81 (1:1000; Invitrogen, cat. R10367), E1A (1:1000; BD Pharmingen, cat. 554155; San Jose, CA, USA), and CD9 (for mouse) (1:1000; Abcam, cat. ab82390; Cambridge, UK). The membranes were then washed in buffer and incubated with secondary antibodies for 1 h at room temperature. After further washing, the membranes were visualized using the Amersham ECL chemiluminescence system (GE Healthcare UK Ltd.).

Quantitative polymerase chain reaction (qPCR) analysis

Total DNA was extracted from cells using the QIAamp DNA Mini Kit (Qiagen, Valencia, CA, USA) following cell lysis. PCR amplification was performed using 40 cycles of denaturation at 95 °C for 20 s and annealing at 60 °C for 20 s. Data were analyzed using the StepOnePlus real-time PCR system (Applied Biosystems, Waltham, MA, USA). Primers and probes were predesigned by the manufacturer (Applied Biosystems).

The TaqMan E1A probe sequence was 5'-CTGTGTCTAGAGAATGC-MGB-3', and the TaqMan E1A primers were as follows: E1A-F, 5'-CCTGAGACGCCCGACATC-3'; and E1A-R, 5'-GGACCGGAGTCACAGCTATCC-3'

In vivo experiments

All animal experiments were performed in accordance with the protocols approved by the Institutional Animal Care and Use Committee of Okayama University. All experimental procedures adhered to the Animal Research: Reporting of In Vivo Experiments (ARRIVE) guidelines. BALB/c-nu/nu mice and C57BL/6 mice were purchased from CLEA Japan, Inc. Mice were housed in a specific pathogen-free environment in the Department of Animal Resources of Okayama University.

HCT116 cells (1×10^6) and RKO cells (5×10^6) were subcutaneously injected into the flanks of 6-week-old female BALB/c-nu/nu mice. PAN02 cells (1×10^6) were subcutaneously injected into the flanks of 6-week-old female C57BL/6 mice. Treatment was started when the tumors reached a diameter of approximately 5 mm. The perpendicular diameters of each tumor were measured two to three times per week, and tumor volume was calculated using the following formula: tumor volume (mm³) = a × b² × 0.5, where a represents the longest diameter, b represents the shortest diameter, and 0.5 is a constant used to estimate the volume of an ellipsoid.

HCT116 and RKO subcutaneous tumors were injected intratumorally once with OBP-301 (1.0×10^8 PFUs) or PBS, and tumor volume was monitored for up to 28 days after treatment. Whole blood was collected from mice on days 1, 2, 3, 5, and 7 after treatment and subjected to qPCR analysis for serum EV-E1A-DNA (n = 3-4).

In experiments evaluating neutralizing antibodies against adenovirus, 6-week-old female C57BL/6 mice were injected subcutaneously twice with wild-type adenovirus type 5 $(1.0 \times 10^9 \text{ PFUs})$ on days 1 and 8 (n=3-4). Whole blood was collected on days 15, 22, and 29. HCT116 cells $(5.0 \times 10^3 \text{ cells/well in a 96-well plate})$ were

treated with OBP-401 (1 MOI) for 3 days in the presence of serum diluted 1,024-fold, and GFP-positive spots were observed using an Olympus IX71 microscope.

In experiments using C57BL/6 mice immunized with adenovirus, PAN02 subcutaneous tumors were injected intratumorally once with OBP-502 (1.0×10^8 PFUs). Blood samples were collected on days 2, 7, and 14 after treatment, and in vivo monitoring continued through day 28. The correlations between serum EV-E1A-DNA levels on days 2, 7, and 14 and the final tumor volume on day 28 were evaluated. In the survival analysis, a tumor volume of 150 mm³ was defined as the experimental endpoint, and the correlation between EV-E1A-DNA levels on day 2 and the survival period was evaluated.

Statistical analysis

Statistical analyses were performed using JMP software (SAS Institute, Cary, NC, USA). Student's *t*-test was used to assess the significance of differences in continuous variables. *P* values < 0.05 were considered significant.

Data availability

The data generated in this study are available upon request from the corresponding author.

Received: 3 July 2025; Accepted: 29 September 2025

Published online: 04 November 2025

References

- 1. Crowley, E., Di Nicolantonio, F., Loupakis, F. & Bardelli, A. Liquid biopsy: monitoring cancer-genetics in the blood. *Nat. Rev. Clin. Oncol.* 10, 472–484 (2013).
- 2. Nikanjam, M., Kato, S. & Kurzrock, R. Liquid biopsy: current technology and clinical applications. *J. Hematol. Oncol.* 15, 131 (2022).
- 3. O'Driscoll, L. Expanding on exosomes and ectosomes in cancer. N Engl. J. Med. 372, 2359-2362 (2015).
- 4. Thakur, B. K. et al. Double-stranded DNA in exosomes: a novel biomarker in cancer detection. Cell. Res. 24, 766-769 (2014).
- 5. Hoshino, A. et al. Extracellular vesicle and particle biomarkers define multiple human cancers. Cell 182, 1044–1061e1018 (2020).
- 6. Yu, D. et al. Exosomes as a new frontier of cancer liquid biopsy. Mol. Cancer. 21, 56 (2022).
- Sanada, T. et al. Transmission of HBV DNA mediated by Ceramide-Triggered extracellular vesicles. Cell. Mol. Gastroenterol. Hepatol. 3, 272–283 (2017).
- 8. Shalhout, S. Z., Miller, D. M., Emerick, K. S. & Kaufman, H. L. Therapy with oncolytic viruses: progress and challenges. *Nat. Rev. Clin. Oncol.* 20, 160–177 (2023).
- Andtbacka, R. H. et al. Talimogene Laherparepvec improves durable response rate in patients with advanced melanoma. J. Clin. Oncol. 33, 2780–2788 (2015).
- Todo, T. et al. Intratumoral oncolytic herpes virus G47Δ for residual or recurrent glioblastoma: a phase 2 trial. Nat. Med. 28, 1630–1639 (2022).
- 11. Kawashima, T. et al. Telomerase-specific replication-selective virotherapy for human cancer. *Clin. Cancer Res.* **10**, 285–292 (2004).
- 12. Kuroda, S. et al. Telomerase-dependent oncolytic adenovirus sensitizes human cancer cells to ionizing radiation via Inhibition of DNA repair machinery. *Cancer Res.* **70**, 9339–9348 (2010).
- 13. Kanaya, N. et al. Immune modulation by Telomerase-Specific oncolytic adenovirus synergistically enhances antitumor efficacy with Anti-PD1 antibody. *Mol. Ther.* 28, 794–804 (2020).
- 14. Fujiwara, T. Multidisciplinary oncolytic virotherapy for Gastrointestinal cancer. Ann. Gastroenterol. Surg. 3, 396-404 (2019).
- 15. Nemunaitis, J. et al. A phase I study of telomerase-specific replication competent oncolytic adenovirus (telomelysin) for various solid tumors. *Mol. Ther.* **18**, 429–434 (2010).
- Shirakawa, Y. et al. Phase I dose-escalation study of endoscopic intratumoral injection of OBP-301 (Telomelysin) with radiotherapy in oesophageal cancer patients unfit for standard treatments. Eur. J. Cancer. 153, 98–108 (2021).
- Kakiuchi, Y. et al. Local oncolytic adenovirotherapy produces an abscopal effect via tumor-derived extracellular vesicles. Mol. Ther. 29, 2920–2930 (2021).
- 18. Kakiuchi, Y. et al. Exosomes as a drug delivery tool for cancer therapy: a new era for existing drugs and oncolytic viruses. *Expert Opin. Ther. Targets.* 27, 807–816 (2023).
- 19. Wang, Z., Mo, H., He, Z., Chen, A. & Cheng, P. Extracellular vesicles as an emerging drug delivery system for cancer treatment: current strategies and recent advances. *Biomed. Pharmacother.* **153**, 113480 (2022).
- 20. Kalluri, R. & LeBleu, V. S. The biology, function, and biomedical applications of exosomes. Science 367 (2020).

Acknowledgements

The authors would like to thank Ms. Tomoko Sueishi, Ms. Tae Yamanishi, Ms. Yuko Hoshijima, and the Central Research Laboratory of Okayama University Medical School for their excellent technical support. The authors also thank FORTE Science Communications (https://www.forte-science.co.jp/) for English language editing.

Author contributions

C.Y. and S. Kuroda designed the experiments and wrote the manuscript. C.Y. primarily conducted the experiments, with support from S.H., D.K., Y.Y., M.S., Y.H., R.S., T.O., and K.K. S. Kuroda, Y.K., M.H., N.K., S. Kikuchi, S. Kagawa, H.T., and T.F. assisted in the interpretation of the results. Y.U. provided reagents. T.F. supervised the entire project. All authors reviewed and approved the final manuscript.

Funding

This study was supported by AMED Grant Number JP22ck0106569h0003 (Toshiyoshi Fujiwara).

Declarations

Competing interests

Yasuo Urata is the President and CEO of Oncolys BioPharma, Inc., the manufacturer of OBP-301, OBP-401,

(2025) 15:38590

Scientific Reports |

and OBP-502. Hiroshi Tazawa and Toshiyoshi Fujiwara are consultants for Oncolys BioPharma, Inc. The remaining authors declare no competing interests.

Additional information

Supplementary Information The online version contains supplementary material available at https://doi.org/1 0.1038/s41598-025-22389-1.

Correspondence and requests for materials should be addressed to S.K.

Reprints and permissions information is available at www.nature.com/reprints.

Publisher's note Springer Nature remains neutral with regard to jurisdictional claims in published maps and institutional affiliations.

Open Access This article is licensed under a Creative Commons Attribution-NonCommercial-NoDerivatives 4.0 International License, which permits any non-commercial use, sharing, distribution and reproduction in any medium or format, as long as you give appropriate credit to the original author(s) and the source, provide a link to the Creative Commons licence, and indicate if you modified the licensed material. You do not have permission under this licence to share adapted material derived from this article or parts of it. The images or other third party material in this article are included in the article's Creative Commons licence, unless indicated otherwise in a credit line to the material. If material is not included in the article's Creative Commons licence and your intended use is not permitted by statutory regulation or exceeds the permitted use, you will need to obtain permission directly from the copyright holder. To view a copy of this licence, visit http://creativecommons.org/licenses/by-nc-nd/4.0/.

© The Author(s) 2025